


 Cite this: *Chem. Commun.*, 2025, 61, 4265

# Navigating electrochemical oxidative functionalization of olefins: selected mechanistic and synthetic examples

 Chun Qi,<sup>†a</sup> Marharyta Laktsevich-Iskryk <sup>†bc</sup> and Daniele Mazzarella <sup>\*ab</sup>

The functionalization of olefins to form added-value compounds is a cornerstone of modern organic chemistry, promoting the synthesis of complex molecules from simple feedstock materials. In parallel, electrochemistry has emerged as a powerful and sustainable technique for enabling challenging transformations under mild conditions by generating reactive intermediates in a controlled manner. This review highlights recent advances in oxidative electrochemical methods for olefin functionalization, showcasing key developments that underscore the versatility of this approach. Using selected representative examples, we explore diverse mechanistic pathways, bond-forming strategies, and the integration of electrochemical techniques with catalytic systems. By providing a concise overview of this rapidly evolving field, we aim to inspire further innovation in electrochemical methodologies to expand the frontiers of olefin chemistry.

 Received 27th November 2024,  
 Accepted 12th February 2025

DOI: 10.1039/d4cc06306f

[rsc.li/chemcomm](https://rsc.li/chemcomm)

## Introduction

Olefins are among the most versatile and widely utilized building blocks in organic synthesis. Due to the prevalence of carbon-carbon double bonds in feedstock chemicals and natural products, the hydrofunctionalization<sup>1</sup> or difunctionalization<sup>2</sup> of olefins has historically provided efficient and straightforward methods for increasing molecular complexity and forming new chemical bonds. Traditionally, some of these transformations are oxidative in nature<sup>3</sup> and have been achieved under both stoichiometric<sup>4</sup> and catalytic<sup>5</sup> conditions, yielding a wide range of functionalized organic molecules. However, many of these methods rely on reactive electrophilic reagents or chemically aggressive oxidants, which can suffer from low selectivity and pose environmental concerns.

In recent years, electrochemistry has garnered renewed attention as a sustainable and versatile tool for promoting chemical transformations,<sup>6</sup> leveraging electrons to drive radical, polar, and hybrid radical-polar processes. It is therefore unsurprising that electrochemical methods have been increasingly applied to the oxidative functionalization of olefins,<sup>3b,7</sup> offering

a potentially milder and more selective approach compared to traditional methods.

The electrochemical oxidative functionalization of olefins with the reaction partner can occur through various mechanistically distinct pathways, as highlighted in Fig. 1. For example, the olefin can be directly oxidized to its corresponding radical cation, which is then intercepted by nucleophiles. Alternatively, the reaction partner can be anodically transformed into an activated radical/cationic species that subsequently adds to the olefin. These types of transformations could be promoted by the addition of a mediator<sup>8</sup>—a redox-active additive that facilitates the electron transfer event and mitigates issues of electro-degradation by channelling electrons between the electrode and the substrate in a bimolecular fashion. Furthermore, electrochemical transformations can be also conjugated with other catalytic modes of activation such as transition-metal<sup>9</sup> or organocatalysis.<sup>10</sup>



Fig. 1 General representation of the possible oxidative electrochemical pathways for the functionalization of olefins.

<sup>a</sup> Department of Chemical Sciences, University of Padova, Via Francesco Marzolo 1, 35131, Padova, Italy

<sup>b</sup> Department of Chemical Sciences and Technologies, University of Rome Tor Vergata, Via della Ricerca Scientifica 1, 00133, Rome, Italy.  
 E-mail: [daniele.mazzarella@uniroma2.it](mailto:daniele.mazzarella@uniroma2.it)

<sup>c</sup> Department of Chemistry and Biotechnology, Tallinn University of Technology, Akadeemia tee 15, Tallinn 12618, Estonia

<sup>†</sup> These authors have contributed equally.



## Highlight

This review aims to present the state-of-the-art in oxidative olefin functionalization, discussing significant contributions, illustrating different activation modes, and highlighting future challenges within the field. We have organized the review according to the nature of the interaction between the substrate (either the olefin or the reaction partner) and the electrode and categorizing the approaches as either mediated or catalysed.

## Direct oxidation at the anode

As previously discussed, olefins can undergo a direct electron transfer event at the electrode surface, leading to the formation of the corresponding radical cations and, ultimately, functionalized products. In 2018, Cheng and co-workers<sup>11</sup> reported the direct aziridination of tri-substituted styrene derivatives **1** with sulfamate **2** (Fig. 2). The process is performed using graphite felt as the electrode material for both the anode and cathode under potentiostatic conditions. Additionally, LiClO<sub>4</sub> served as the electrolyte, and 2,6-lutidine as a basic additive in acetonitrile. The authors propose a reaction mechanism where the olefin **1** is anodically converted into radical cation **4**, which is subsequently attacked by sulfamate **2** to generate radical intermediate **5**. This neutral species is then oxidized at the anode to produce carbocation **6**, which cyclizes to form the desired aziridine product **3**. Finally, cathodic hydrogen evolution completes the electrochemical process. The scope of this reaction is broad as a wide variety of styrene derivatives can be electrochemically converted into the corresponding aziridines. However, this protocol appears to be restricted to the use of sulfamate **2** as the nucleophilic partner.

In 2021, this limitation was overcome by the group of Noël,<sup>12</sup> who reported a flow electrochemical procedure for the aziridination of styrene derivatives **7** with a wide range of primary amines **8** as nucleophiles (Fig. 3). The use of flow technology<sup>13</sup> was crucial, as it enabled the formation of the target aziridine



Fig. 3 Electrochemical aziridination of internal alkenes with primary amines. Blue electrode: cathode; red electrode: anode.

in a very short residence time (5 minutes), thus preventing the electrochemical degradation of product **9** observed under batch conditions. The process employs graphite and iron as the anodic and cathodic materials, respectively, under galvanostatic conditions in acetonitrile. Hexafluoroisopropanol was used as the proton source, while  $\gamma$ -terpinene was added to prevent further oxidation of the aziridine product.

A similar electrochemical approach for constructing the aziridine core was demonstrated by the Cheng group in the same year, utilizing batch conditions and a constant potential mode of electrolysis.<sup>14</sup> However, in this case, the substrate scope was limited to the use of ammonia as nucleophile.

The oxidative electrochemical functionalization of olefins is not solely represented by C–N bond formation; dialkoxylation processes have also been reported. For instance, in 2019, Xu, Zhang and co-workers<sup>15</sup> described a direct electrochemical dimethoxylation of styrenes (Fig. 4). This protocol uses platinum



Fig. 2 Electrochemical aziridination by alkene activation using a sulfamate as the nitrogen source. HfsNH<sub>2</sub>; 1,1,1,3,3,3-hexafluoro-2-propyl sulfamate. GF: graphite felt; blue electrode: cathode; red electrode: anode.



Fig. 4 Substrate-dependent electrochemical dimethoxylation of olefins. Blue electrode: cathode; red electrode: anode.



as both cathodic and anodic material under galvanostatic conditions and was carried out at 60 °C in a mixture of acetonitrile and methanol, with  $n\text{Bu}_4\text{NBF}_4$  as the electrolyte. This method can generate different products based on the structure of the olefin.

The authors propose that these variations arise from the differences in stability of the carbocationic intermediates formed during the electrochemical oxidation. In the case of trisubstituted styrenes **11**, the stable tertiary carbocation **14** undergoes nucleophilic addition by methanol.

In contrast, with disubstituted stilbene derivatives **10**, the secondary carbocation **15** undergoes a semi-pinacol rearrangement to form acetal product **12**. In a similar fashion, the group of Yoshida<sup>16</sup> reported an electrochemical strategy to convert styrene derivatives **17** into the corresponding 1,2-diketones **18** (Fig. 5). In this case, dimethyl sulfoxide (DMSO) acts as a trapping agent, ultimately forming oxysulfonium ion intermediate **19**, which is then treated with triethylamine to yield the corresponding diketone product **18**. In contrast to classical chemical oxidations, such as those using  $\text{RuCl}_3/\text{NaIO}_4$ ,<sup>17</sup> this approach prevents the cleavage of carbon–carbon bonds.

The functionalization of olefins can also proceed with diverse nucleophiles, allowing access to a variety of hetero 1,2-difunctionalized products.

For instance, the group of Moeller has conducted extensive work in this area.<sup>18</sup>

In their seminal contribution in 1991,<sup>18a</sup> they described an intramolecular anodic olefin coupling cyclization reaction involving enol ethers decorated with a pendant olefinic moiety **20** that served as the intramolecular first nucleophilic trap and methanol as the second nucleophile (Fig. 6).

The process relies on the use of platinum as both the anodic and cathodic material,  $\text{LiClO}_4$  as the electrolyte, and lutidine as the base in a solvent mixture of  $\text{MeOH}/\text{CH}_3\text{CN}$  or  $\text{MeOH}/\text{THF}$ . A variable current of 10–12 mA was applied, depending on the substrate. From a mechanistic standpoint, the reaction begins with the oxidation of the electron-rich enol ether moiety,



Fig. 5 Integrated electrochemical-chemical oxidation mediated by alkoxysulfonium ions. CF: carbon felt; blue electrode: cathode; red electrode: anode.



Fig. 6 Intramolecular anodic olefin coupling reactions: a method for carbon–carbon bond formation. Blue electrode: cathode; red electrode: anode.

leading to radical cation **22** that subsequently cyclizes onto the pendant olefin fragment. The resulting radical cation **23** undergoes a sequence of single electron oxidation and trapping by  $\text{MeOH}$  to furnish the targeted cyclic product **21**. Later, the same group extended this oxidative approach to a variety of other substrates as well as to the formation of C–N bonds.<sup>18b–g</sup>

In addition to intramolecular trapping processes, 1,2-heterodifunctionalizations can also proceed *via* a fully intermolecular mechanism. For example, the group of Xu<sup>19</sup> reported electrochemical carbohydroxylation and carboalkoxylation processes (Fig. 7). These reactions were conducted in an undivided electrolytic cell equipped with a graphite rod anode and a platinum plate cathode at 50 °C, applying a constant current of 5 mA. A solvent mixture of acetonitrile and water was used, with potassium bicarbonate serving as basic additive. The reaction mechanism commences with the anodic oxidation of olefin **24** to generate radical cation **27**, which is then captured



Fig. 7 Electrochemically enabled carbohydroxylation of alkenes with  $\text{H}_2\text{O}$  and organotrifluoroborates. GR: graphite rod; blue electrode: cathode; red electrode: anode.



## Highlight

by the organic trifluoroborate reagent **25** to form radical intermediate **28**. Subsequently, **28** is further oxidized to form carbocation **29**, which then reacts with H<sub>2</sub>O to yield the final alcohol product **26**.

## Oxidation of the reaction partner

Another possible mechanistic scenario involves the anodic oxidation of the reaction partner (Fig. 8), generating a radical species that subsequently reacts with the olefin to form a second radical intermediate. Oxidation of the latter produces a carbocation, which can then be intercepted by a nucleophilic partner to yield the difunctionalized product.

Several radical precursors have been employed in this area to enable such transformations. Among them, the Langlois reagent—a commonly used precursor for producing CF<sub>3</sub> radicals under oxidative conditions<sup>20</sup>—has been extensively used in electrochemical settings by several groups.<sup>21</sup> For instance, the group of Cantillo and Kappe<sup>22</sup> demonstrated the use of this reagent with styrene derivatives **30** as the olefin partner and water as the nucleophile, yielding oxo-trifluoromethylated compounds of the type of **31**. Similarly, the group of Lei<sup>23</sup> has reported an analogous transformation, expanding the scope to include other oxygen and nitrogen-centered nucleophiles. These transformations can also occur intramolecularly. The group of Xu<sup>24</sup> employed styrene derivative **32** bearing a pendant nucleophilic handle, such as a carboxylic acid, to induce intramolecular nucleophilic attack, leading to the synthesis of trifluoromethylated lactone derivatives of the type of **33**. In 2019, the research group of Chen and Zhang<sup>25</sup> reported the electrochemical trifluoromethylation of vinyl cyclobutanol **34**, followed by a pinacol rearrangement to yield ketone structures as **35**. Lei<sup>26</sup> and co-workers further expanded this strategy by reporting various migrating groups, including different alkyl and aryl groups, in the electrochemical trifluoromethylation of

propylene alcohol *via* 1,2-carbon migration. Beyond the Langlois reagent, other sulfonyl derivatives have been used as radical precursors. As a representative example, the group of Lei<sup>27</sup> has reported the use of sulfonyl hydrazides as precursors to sulfonyl radicals, promoting the difunctionalization of styrene compounds **36** in the presence of an alcohol nucleophile, affording  $\beta$ -alkoxy sulfones **37**. Independent work by the groups of Lei<sup>28</sup> and Pan<sup>29</sup> further broadened the types of sulfur-based radicals employed in these transformations to thiols. Thiols can be deprotonated and oxidized to yield radical intermediates, which were subsequently employed to difunctionalize olefin **38** in combination with oxygen- or nitrogen-centered nucleophiles. Building on this approach, the group of Chen and Lei<sup>30</sup> further extended this methodology to diselenides, enabling the anodic generation of selenyl radicals. Similarly to their sulfur-based counterparts, these open-shell species participate in addition reactions with styrene partner **40**, yielding the corresponding difunctionalized product **41**.

The aforementioned transformations predominately rely on a radical precursor and a nucleophile to achieve olefin difunctionalization. However, in 2019, Lam and co-workers<sup>31</sup> demonstrated that oxidative difunctionalization could also proceed *via* the addition of two open-shell species onto an olefin (Fig. 9).

This protocol was carried out between hemioxalate ammonium salts of the type of **42** as both the olefin and the radical source and aliphatic carboxylic acids **43**, in an electrochemical cell equipped with two platinum electrodes. The reaction was performed in methanol as the solvent, with potassium hydroxide as a basic additive, under constant current electrolysis at room temperature. Under these conditions, substrate **42** undergoes anodic decarboxylation, generating oxycarbonyl radical **45**, which undergoes a 5-*exo*-trig cyclization to form alkyl radical **46**. Concomitantly, a deprotonation–oxidation sequence converts carboxylic acid **43** into alkyl radical **47**, which couples with the previously formed radical **46** to yield the desired lactone product **44**.

On top of single-electron oxidation, other radical-generating pathways can be operative under electrochemical conditions. For instance, in 2021, the group of He<sup>32</sup> demonstrated



Fig. 8 Examples of the anodic difunctionalization of olefins enabled by the oxidation of the reaction partner to a radical intermediate.



Fig. 9 Route towards substituted lactones by anodic generation of oxycarbonyl radicals. Blue electrode: cathode; red electrode: anode.





Fig. 10 Electrochemical radical silyl-oxygenation of activated alkenes. Blue electrode: cathode; red electrode: anode.

the 1,2-silyloxygenation of electron-poor olefin **50** using a *N*-hydroxy compound **48** in combination with a silane reaction partner **49** (Fig. 10). This process was performed at constant current in an undivided cell equipped with a graphite anode and a platinum cathode, using  $\text{LiClO}_4$  as the electrolyte and a solvent mixture of acetone and acetonitrile. Mechanistically, the reaction begins with an anodic proton-coupled oxidation of *N*-hydroxy compound **48**, leading to *N*-oxyl species **52**. Radicals of the type of **52** are well-known radical generators through a hydrogen atom transfer (HAT) mechanism.<sup>33</sup> This type of process with silane **49** generates the corresponding silyl radical **53**, which adds to olefin **50** to generate electrophilic radical **54**. Finally, radical–radical coupling of **54** with a second *N*-oxyl species **52** forms the target difunctionalized product **51**. Notably, this method was also extended to include the 1,2-germanyloxygenation by replacing the silane with a germane compound.

Not only radical pathways are available for the electrochemical difunctionalization of olefins. In 2002, Yudin<sup>34</sup> and co-workers reported an electrochemical aziridination process involving aminophthalimide **55** and several olefins **56** (Fig. 11). Crucially, mechanistic studies<sup>35</sup> detailed that electrochemically



Fig. 11 Olefin aziridination with a broad substrate scope. Blue electrode: cathode; red electrode: anode.



Fig. 12 Oxidative generation of diarylcarbenium ion pools. CF: carbon felt; blue electrode: cathode; red electrode: anode.

generated nitrenes served as pivotal reaction intermediates. In this case, the reaction is performed in a divided cell under potentiostatic conditions, using platinum as both the anodic and cathodic material, with a  $\text{Et}_3\text{N}/\text{AcOH}$  mixture as electrolyte and acetonitrile as the solvent.

Notably, this electrochemical method can be applied to a variety of electron-rich and electron-deficient olefins, efficiently converting them into aziridines.

Besides open-shell and carbene intermediates, carbocations can also participate in olefin functionalization. In 2006, the group of Yoshida<sup>36</sup> reported the oxidative formation of diaryl carbocations, which were then used in combination with a nucleophilic olefin partner (Fig. 12).

The protocol was conducted in a divided electrolytic cell equipped with a carbon felt anode and platinum cathode, under constant current conditions at  $-78^\circ\text{C}$ . Dichloromethane was used as the solvent, and  $n\text{Bu}_4\text{NBF}_4$  served as the electrolyte. During the reaction, diarylmethane **58** is anodically oxidized to form a  $\pi$ -delocalized radical cation intermediate **61**, which is deprotonated to form benzyl radical **62**. A subsequent anodic step converts this open-shell species into the corresponding diaryl carbocation **63**, which is then intercepted by nucleophilic olefins such as allyl silanes and silyl enol ether **59**, affording the desired product **60**.

Cationic intermediates were also proposed in the electrochemical strategy for the Markovnikov azidoiodination of alkenes, reported by the group of Zeng<sup>37</sup> in 2017 (Fig. 13). The reaction was carried out using graphite plates as both the cathode and anode in a divided electrochemical cell, under constant-current electrolysis, in a solution of  $\text{LiClO}_4$  in MeOH (or MeOH/ $\text{H}_2\text{O}$ ). Mechanistically, the anodic oxidation of iodide from either  $\text{NaI}$  or  $\text{NH}_4\text{I}$  generates molecular iodine, which then reacts with sodium azide to form  $\text{IN}_3$ . The use of a polar solvent was essential for the formation of Markovnikov products, as it promotes heterolytic rather than homolytic bond cleavage of  $\text{IN}_3$  to produce  $[\text{I}^+]$  and  $\text{N}_3^-$ . The resulting electrophilic iodine species react with the alkene to produce cyclic iodonium intermediate **66**, which undergoes nucleophilic ring opening by the azide anion producing vicinal iodoazides **65**.

Taking a different approach but aligned with the broader goal of harnessing electrophilic halogen species for olefin



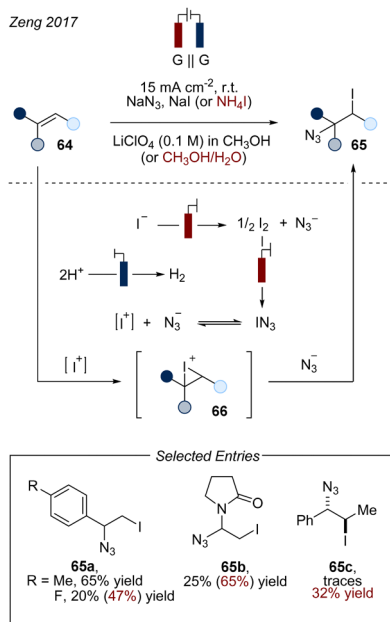


Fig. 13 Electrochemical azidoiodination of alkenes. Blue electrode: cathode; red electrode: anode.

functionalization, Waldvogel and Morandi<sup>38</sup> proposed the use of 1,2-dihalogenated ethane as a source of both electrophilic and nucleophilic halogen species for the vicinal dihalogenation of olefins (Fig. 14). In this approach, the reduction of 1,2-dibromoethane on the graphite cathode generates an alkyl radical **71** and bromide anion. The Br<sup>-</sup> is then oxidized on the graphite anode yielding [Br<sup>+</sup>], which subsequently reacts with the alkene to form intermediate **70**. At the same time, further cathodic reduction of carbon radical **71** produces an

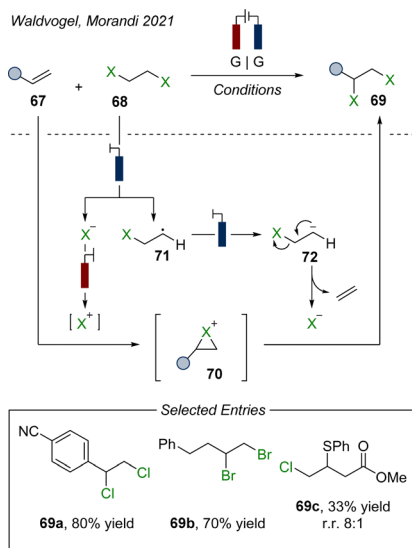


Fig. 14 Electrochemical dihalogenation of alkenes. Conditions: X = Br or X = Cl, SPh: 10 mA cm<sup>-2</sup>, 3–16 F, HFIP (1 vol%), Et<sub>4</sub>NBF<sub>4</sub> (0.2 M), r.t., CH<sub>3</sub>CN, N<sub>2</sub>. X = Cl: 4 mA cm<sup>-2</sup>, 2.5–9 F, MnCl<sub>2</sub>·4H<sub>2</sub>O (5 mol%), Et<sub>4</sub>NBF<sub>4</sub> (0.1 M), 50 °C, CH<sub>3</sub>CN, N<sub>2</sub>. Blue electrode: cathode; red electrode: anode.

additional bromide anion capable of opening the ring of **70** and producing the 1,2-dibrominated products with the release of ethylene as a byproduct.

Cyclic voltammetry studies indicate that adding HFIP to the reaction system plays a crucial role in preventing unproductive polymerization of the alkene at the cathode. It was also shown that the proposed transformation is feasible for the retro-dihalogenation of polyhalogenated compounds. For instance,  $\gamma$ -hexachlorocyclohexane, known as a persistent pollutant, was fully dechlorinated in the presence of an acceptor alkene, yielding benzene. This demonstrates that the developed approach has the potential to recycle persistent pollutants into valuable chemical reagents, providing a sustainable pathway for repurposing environmentally harmful substances.

## Use of redox mediators

Redox mediators are well-established and versatile tools in electrochemical transformations, offering several key advantages.<sup>8</sup> These additives facilitate selective oxidation or reduction processes by channelling electrons between the electrode and the substrate. This not only mitigates kinetic inhibition but also protects substrates from overoxidation.<sup>8</sup> Such capabilities are particularly valuable in olefin transformations, where mediators help prevent issues like uncontrolled polymerization and electrode passivation. Moreover, mediators enhance reaction selectivity and protect sensitive functionalities, thereby broadening the substrate scope. Among the various mediation strategies, halogen-based electrochemical mediation stands out for its simplicity and versatility.<sup>39</sup> This approach uses readily available, cost-effective, and non-toxic reagents, such as MX salts (M = K, Na, Mg, etc.), NH<sub>4</sub>X, or NR<sub>4</sub>X, which serve a dual role as halogen sources and electrolytes in the electrochemical system. Notably, this method is adaptable to both in-cell and ex-cell modes of electrosynthesis, further increasing its applicability across diverse electrochemical setups. Mechanistically, halogen mediation typically involves the anodic oxidation of the halogen source, generating electrophilic halogen species ([X<sup>+</sup>]).

These species may exist as neutral molecules (X<sub>2</sub>), halogen radicals (X<sup>•</sup>), or partially positively charged species (e.g., HOX or <sup>-</sup>OX). These electrophilic intermediates can interact with electron-rich olefins or reactive intermediates, driving product formation.

An illustrative example of this approach in the area of olefin functionalization was reported in 2019 by the Waldvogel group.<sup>40</sup> They employed anodic oxidation of 4-methyliodobenzene in the presence of Et<sub>3</sub>N·5HF to generate a fluorinated hypervalent iodine mediator **75** *in situ*, enabling the intramolecular cyclization of *N*-benzamides **73** into fluoromethylated oxazolines **74** through the formation of iodonium species **76** (Fig. 15). The reaction was performed in undivided cell utilizing two platinum electrodes and maintaining a constant current density of 50 mA cm<sup>-2</sup>.

For certain starting compounds (e.g. **73c**) higher yields were obtained using an ex-cell approach, where the amide substrate was introduced into the reaction mixture after the electrochemical generation of ArIF<sub>2</sub>. Nevertheless, due to the low stability





Fig. 15 Electrochemical fluorocyclization of *N*-allylcarboxamides to 2-oxazolines by hypervalent iodine mediator. Blue electrode: cathode; red electrode: anode.

of the  $I(III)$  species, this approach proved ineffective in most cases.

More recently, de Vos and co-workers reported an electrochemical bromide-mediated olefin epoxidation strategy (Fig. 16).<sup>41</sup>

Sodium bromide was employed as the halogen source for the anodic production of electrophilic bromine species, which then reacts with olefin **78** to form cyclic bromonium **80**. This intermediate undergoes ring opening *via*  $OH^-$ , generated through cathodic reduction of water, producing bromohydrin **81**. A subsequent intramolecular  $S_N2$  reaction converts **81** into epoxide products **79**, while regenerating  $Br^-$  to complete the catalytic cycle. The reaction was performed in an undivided cell using two platinum electrodes under constant current, with



Fig. 16 Bromide mediated electrochemical olefin epoxidation. Blue electrode: cathode; red electrode: anode.

$Et_4NBF_4$  as the electrolyte in a  $CH_3CN/H_2O$  solvent system. The nature of electrolyte, as well as its optimal proportion relative to  $NaBr$ , was crucial in suppressing the undesired formation of the dibrominated product. In a model experiment, the optimal yield of the epoxide product was achieved at a  $NaBr/Et_4NBF_4$  ratio of 1.5 : 2. The authors attributed this effect to the electrolyte's ability to create a specific microenvironment around the bromonium ion, effectively shielding it from nucleophilic attack by  $Br^-$ .

Halogen-based electrochemical mediation was also applied to semi-pinacol rearrangement, as described by the Onomura group in 2019 using  $\alpha,\alpha$ -disubstituted allyl alcohols as **82** (Fig. 17).<sup>42</sup>

The reaction begins with the formation of cyclic halonium ion **84** from anodically generated chlorine or bromine and the double bond. Deprotonation of the hydroxyl group within **84** by cathodically generated alkoxide triggers a 1,2-alkyl or aryl shift, accompanied by halonium ion ring opening. This step is followed by dehydrohalogenation of **85**, yielding  $\alpha$ -*exo*-methylene ketones **83**. The reaction employed two platinum electrodes, with electrolysis conducted at 0 °C under a constant current of 50 mA, using an inorganic salt as both the halogen source and electrolyte. For aromatic cyclic allylic alcohols,  $CaCl_2$  in a  $MeOH/CH_3CN$  solvent system provided optimal conditions, while acyclic substrates were converted with higher efficiency using  $CaBr_2 \cdot H_2O$  in a  $CF_3CH_2OH/CH_3CN$  mixture. For alkyl-substituted substrates, the best results were achieved with  $MgCl_2$ , supplemented by excess 1,8-diazabicyclo[5.4.0]undec-7-ene (DBU) to facilitate the final dehydrohalogenation step.

This mediation approach is not only restricted to the use of halides. In 2021, the Wickens group introduced an ex-cell protocol for constructing aziridines *via* the formation of a metastable dicationic adduct between alkene **86** and anodically



Fig. 17 Synthesis of  $\alpha$ -*exo*-methylene ketones from  $\alpha,\alpha$ -disubstituted allyl alcohols by electrochemical oxidative migration. Blue electrode: cathode; red electrode: anode.





Fig. 18 Aziridine synthesis by coupling amines and alkenes via an electrogenerated dication. Blue electrode: cathode; red electrode: anode.

oxidized thianthrene (Fig. 18) in a divided cell.<sup>43</sup> Unlike the aforementioned strategies developed by Noël<sup>12</sup> and Cheng,<sup>11</sup> this transformation targeted non-activated monoalkyl-substituted alkenes within its substrate scope. This was accomplished by decoupling the oxidative alkene activation and the aziridination steps. Upon anodic oxidation, thianthrene **TT** is converted into cation radical  $\text{TT}^{\bullet+}$ , which could react with alkene **86**, producing two distinct dicationic species. Sequential additions of two  $\text{TT}^{\bullet+}$  to the double bond resulted in the formation of the bis-adduct **89**, while the mono-adduct **90** was formed *via* cycloaddition between the thianthrenium dication  $\text{TT}^{2+}$ , generated through a disproportionation reaction, and the alkene. Subsequent treatment of these intermediates with an amine in the presence of  $\text{Cs}_2\text{CO}_3$  yielded the target aziridine products **88**.

Similar to the vicinal dihalogenation strategy previously described by Waldvogel and Morandi,<sup>38</sup> in 2021, Lei and coworkers<sup>44</sup> utilized dichloroethane (DCE) as an inexpensive bulk material for the cathodic generation of chloride anions that were later used as mediators in the anodic synthesis of oxazolines **93** (Fig. 19). Onium intermediate **94**, formed upon the interaction of olefin **91** with electrophilic chlorine species, can be intercepted by amides, followed by an intramolecular displacement of the halide. This strategy enabled the efficient transformation of a broad scope of styrene-type alkenes and amides into the corresponding oxazolines **93** through constant-current electrolysis in DCE at 80 °C. The reaction employed a carbon block anode, a nickel cathode, and  $n\text{Bu}_4\text{NPF}_6$  electrolyte.

In addition to affording onium compounds for olefin activation, iodine has also been used for the electrochemical activation of the coupling partner.



Fig. 19 Electrochemical (3+2) cyclization between amides and olefins. Blue electrode: cathode; red electrode: anode.

Yuan's group<sup>45</sup> and Terent'ev's group<sup>46</sup> independently reported iodide-mediated electrochemical synthesis of vinyl sulfones from sodium sulfinates and sulfonyl hydrazides, respectively (Fig. 20). In these transformations, inorganic iodates served as substrates for anodic oxidation, generating electrophilic iodine species that interacted with sulfinates or hydrazides to yield sulfonyl iodide **99**. Depending on the reaction conditions, S-centered radical **101** is generated either through the direct homolytic bond cleavage of **99** (conditions A), or *via* cathodic reduction of **99**, followed by a one-electron oxidation of the resulting anion **100** (conditions B).

Radical addition of **101** to styrene-type alkenes produces a C-centered radical **102**, which could then be trapped by an iodine radical or anodically oxidized in the presence of iodide. The resulting iodosulfone **103** liberates HI, yielding the target product **98**. Another approach using halogen mediation in electrochemical transformations involves the interaction of electrophilic halogen species with reaction intermediates generated after the addition of a coupling partner to electron-deficient alkenes. This approach was used by the Elinson group<sup>47</sup> in 2000 for constructing cyclopropane cores from dialkyl malonates **104** and alkylideneacyanoacetates **105** (Fig. 21). The protocol relies on the preliminary deprotonation of malonate by the ethoxide anion, generated through the reduction of ethanol solvent on a stainless steel cathode.

The nucleophilic addition of deprotonated malonate **107** to the electron-deficient double bond within **105** produces carbanion **108**, which subsequently interacts with electrophilic bromine generated on the graphite anode. The resulting brominated intermediate **109** undergoes further deprotonation, triggering an intramolecular ring closure to form the cyclopropane core in a highly stereoselective manner, with



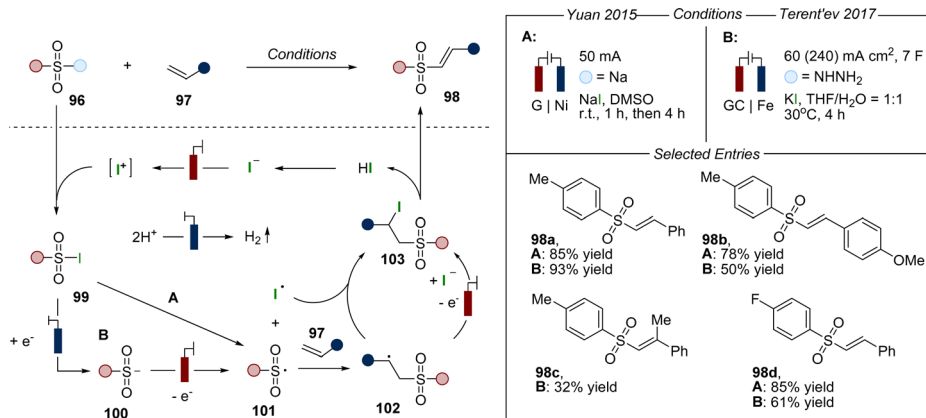


Fig. 20 Iodine-promoted electrocatalytic synthesis of vinyl sulfones from alkenes. Blue electrode: cathode; red electrode: anode.

the release of a bromide anion. Although the substrate scope of this transformation was initially narrow, this approach proved to be efficient and was further extended to an enantioselective organocatalytic version by the Ošeka group<sup>48</sup> in 2024.

Dicarbonyl compounds can also add on electron-rich or electron-neutral carbon-carbon double bonds upon single electron oxidation. Specifically, the group of Xu<sup>49</sup> exploited phenothiazine **112** as a redox mediator for the electrochemical synthesis of *N*-heterocyclic compounds of the type of **113** and **114** via the dehydrogenative annulation of *N*-allyl amides **110** and 1,3-dicarbonyl compounds **111** (Fig. 22).

In the proposed reaction system, oxidation of **112** at the RVC anode produces the corresponding radical cation, which serves as a single-electron acceptor on the key steps of the transformation. Concurrent water reduction at the platinum cathode provides mildly basic conditions. The reaction proceeds through a complex mechanism involving the initial deprotonation of 1,3-

dicarbonyl compound **111** to anion **115**, followed by its oxidation to C-centered radical **116**. The latter undergoes addition to the double bond of **110**, producing tertiary radical **117**. Further **112**-mediated oxidation and intramolecular cyclization delivers **118**, which undergoes hydroxylation and C–N bond cleavage to afford intermediate **120**. Depending on the structure of the starting dicarbonyl compound, **120** could be transformed into two different products. Methoxy-substituted substrates **111** deliver the pyrrolidine product **113** through a **112**-promoted C(sp<sup>3</sup>)-H/N–H cross-coupling reaction, while **120** derives from an alkyl acetoacetate undergoing intramolecular dehydration to form tetrahydropyridine **114**.

Mediated electrocatalysis was also applied in the field of polymerization.<sup>50</sup> In 2018 the groups of Lin and Fors<sup>51</sup> reported the use of TEMPO as a mediator for the electrochemical cationic polymerization of vinyl ethers **122** (Fig. 23). TEMPO was exploited as a redox mediator to prevent the uncontrolled polymerization process attributed to the irreversible oxidation of the dithiocarbamate chain transfer agent (CTA) occurring upon direct electrolysis. The reaction proceeded in a divided cell with two RVC electrodes under galvanostatic conditions, with *n*Bu<sub>4</sub>NClO<sub>4</sub> as the electrolyte, and dichloromethane as the solvent. Mechanistic studies suggested that TEMPO undergoes anodic oxidation to form a cation that is trapped by the CTA, producing stabilized cation **124**. Fragmentation of **124** regenerates TEMPO, producing dithiocarbamate radical **125** along with oxocarbenium ion, which participates in the polymerization step. Notably, by reversing the current in the electrochemical cell, **125** is reduced to its anionic form, which caps the propagating polymer cation, enabling precise electrochemical control over the chain growth of the polymer.



Fig. 21 Stereoselective electrocatalytic transformation of alkylidenecyanoacetates and malonate into (*E*)-3-substituted-2-cyanocyclopropane-1,1,2-tricarboxylates. Blue electrode: cathode; red electrode: anode.

## Catalytic electrochemical transformations of olefins

Another approach to facilitate electrochemical reactions is the use of catalysts. Unlike mediators, catalysts do not typically channel electrons between the electrode and the substrate, but instead accelerate reactions by lowering the activation energy.





Fig. 22 Synthesis of N-heterocycles via dehydrogenative annulation of *N*-allyl amides with 1,3-dicarbonyl compounds. Blue electrode: cathode; red electrode: anode.

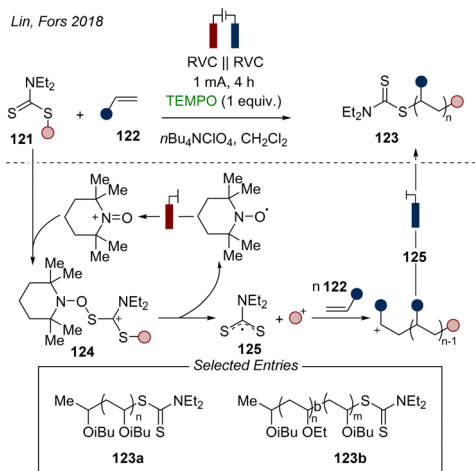


Fig. 23 Electrochemically controlled cationic polymerization of vinyl ethers. Blue electrode: cathode; red electrode: anode.

Catalysts and mediators can even function synergistically within the same reaction system.

In the area of alkene difunctionalization, in 2017, the Lin group<sup>52</sup> disclosed a manganese(II)-promoted electrochemical diazidation of olefins (Fig. 24). The transformation was conducted using an RVC anode, a Pt cathode, acetic acid as an additive, and LiClO<sub>4</sub> as the electrolyte. Electrolysis of the reaction components in CH<sub>3</sub>CN was performed under a constant potential of 2.3 V. The reaction proceeds *via* sequential addition of two azido radicals to olefin **126**. However, direct anodic generation of the azido radical leads to undesirable side reactions, yielding only trace amounts of the diazidated product. To achieve better control, MnBr<sub>2</sub>·4H<sub>2</sub>O was employed as a catalyst. Indeed, manganese(II) can form a complex with the azide anion and, upon anodic oxidation, generates azido metal adduct Mn(III)-N<sub>3</sub>. This intermediate can add to both the double bond of the substrate and the monoazidated

intermediate **128** producing target diazidated products **127**. This approach was further expanded to Mn(II)-promoted electrochemical dichlorination,<sup>53</sup> chlorotrifluoromethylation,<sup>54</sup> and chloroalkylation of olefins.<sup>55</sup>

In a complementary approach, the group of Park<sup>56</sup> demonstrated that anodically generated azido radicals can function as HAT agents, providing an efficient protocol for the C(sp<sup>3</sup>)-H functionalization of  $\gamma$ -lactams (Fig. 25).

The azido radical abstracts a hydrogen atom from **129**, generating a nucleophilic  $\alpha$ -amino radical **132** that can react with electron-deficient alkene **130**. A subsequent HAT event, from either substrate **129** or the solvent, completes the transformation, yielding the final product **131**. In the reaction system, a catalytic amount of the azide ion source, *n*Bu<sub>4</sub>NN<sub>3</sub>, was used along with a glassy carbon anode, a carbon felt cathode, and CH<sub>3</sub>CN as the solvent.



Fig. 24 Metal-catalyzed electrochemical diazidation of alkenes. Blue electrode: cathode; red electrode: anode.





Fig. 25 Electrochemical C(sp<sup>3</sup>)-H functionalization of  $\gamma$ -lactams based on hydrogen atom transfer. GF: graphite felt; blue electrode: cathode; red electrode: anode.

Electrochemical tools can be also employed in the area of transition-metal-catalyzed C-H activation.<sup>57,58</sup> The group of Ackermann<sup>59</sup> used a cost-effective  $\text{Co}(\text{OAc})_2$  catalyst to promote oxidative allene annulation, exploiting a simple electrochemical system consisting of a RVC anode, a Pt cathode, NaOPiv as basic additive, and MeOH as the solvent (Fig. 26).



Fig. 26 Electrooxidative allene annulations by mild cobalt-catalyzed C-H activation. Blue electrode: cathode; red electrode: anode.

The protocol was demonstrated to deliver products in high yields with excellent regioselectivity. This was rationalized by mechanistic studies, which indicated that migratory allene insertion into the Co-C bond of intermediate **137**, formed upon carboxylate-assisted C-H/N-H activation of **134** by the anodically generated Co(III) catalyst, proceeds at the distal position to the allene substituent due to lower energy requirements. The resulting intermediate **138** undergoes reductive elimination with the formation of a Co(I) species, which is then subjected to anodic oxidation to regenerate the Co(II) catalyst. The resulting *exo*-methylene isoquinolone **139** is converted into the final product **136** via base-promoted isomerization. The same group later expanded this work by developing asymmetric versions of this metallaecatalytic approach, such as the cobalt-catalyzed C-H annulation with allenes for the synthesis of atropochiral and P-stereogenic compounds,<sup>60</sup> as well as the enantioselective C-H annulation of benzoic acid derivatives with acrylates.<sup>61</sup>

Metal complexes can serve not only to enable cross-coupling reactions but also as Lewis acid catalysts to promote electron transfer on the target substrate. In 2019, the Meggers group<sup>62</sup> reported the use of a Rh-based chiral complex<sup>63</sup> to serve both as the electrocatalyst and source of asymmetric induction in the coupling of 2-acyl imidazoles **140** with silyl enol ethers **141** (Fig. 27). The initial steps of this transformation involve the base-assisted formation of Rh-bonded enolate **144** from **140** and  $\Delta\text{-Rh2}$ , followed by its anodic oxidation to radical



Fig. 27 Electrocatalytic cross-coupling of 2-acyl imidazoles with silyl enol ethers promoted by chiral Rh complex. Blue electrode: cathode; red electrode: anode.





Fig. 28 Electrochemical asymmetric radical functionalization of aldehydes enabled by a redox shuttle. Blue electrode: cathode; red electrode: anode.

intermediate **145**. The crystal structure of **144** revealed a strong *re*-face shielding by trimethylsilyl substituent, which governs the highly stereoselective radical addition of **141** to **145**, leading to the formation of a second radical intermediate **146**.

Radical species **146** then undergoes an anodic oxidation-desilylation-ligand exchange sequence to produce the final product **142**. By modifying the reaction conditions and introducing ferrocene as redox mediator into the electrochemical system, the scope of this protocol was expanded to potassium alkenyl trifluoroborate partners.<sup>64</sup>

Merging electrochemistry with asymmetric aminocatalysis has gained significant interest due to its sustainable approach to enantioselective transformations, offering novel methods under mild conditions.<sup>65</sup> However, the oxidative degradation of aminocatalysts remains a major challenge for the advancement of this methodology. Recently, our group<sup>66</sup> proposed a potential solution by developing a redox shuttle<sup>67</sup>-controlled asymmetric alkylation of aldehydes **148** with silyl enol ethers **149** (Fig. 28). The reaction utilizes an RVC anode and a stainless steel cathode under galvanostatic conditions, with aminocatalyst **I** and redox additive **150** as key components. The process is conducted in dichloromethane, with nBu<sub>4</sub>NClO<sub>4</sub> as the electrolyte, and HFIP and H<sub>2</sub>O as protic additives. Mechanistic studies revealed that the enamine intermediate **152**, arising from the

condensation of aldehyde **148** and aminocatalyst **I**, undergoes anodic oxidation to form radical cation **153**. This intermediate is then trapped by silyl enol ether **149**, resulting in the formation of a new radical cation intermediate **154**. A second anodic oxidation leads to the target product **151** after hydrolysis. Initial low product yields were significantly improved by introducing biphenyl derivative **144** into the reaction system, which effectively controlled the cell potential, thereby preventing the unproductive degradation of the aminocatalyst.

## Conclusions

In recent years, significant progress has been made in advancing the electrochemical functionalization of olefins, with numerous research groups developing innovative strategies to harness electrochemical methods. This review has summarized key approaches in the field, including the direct electrochemical activation of olefins and their reaction partners, as well as the development of mediated and catalytic systems that enhance versatility and control.

Looking ahead, future research in electrochemical olefin functionalization should focus on expanding the range of bond formations, particularly for constructing C–P and C–B bonds, which are vital in pharmaceuticals, materials science, and agrochemistry. Further advancements in transition-metal catalysis and organocatalysis will be essential for improving reaction efficiency, selectivity, and functional group compatibility. Complementary fields, such as electrochemically driven biocatalysis, also offer exciting potential for enabling highly selective and sustainable transformations under mild conditions, thereby broadening the applicability of these methods. Moreover, the possibility to dose the minimum energy required for the desired redox transformation makes electrochemistry an ideal tool to functionalize complex synthetic intermediates in late stage transformation.

In summary, continued exploration of electrochemical approaches to olefin functionalization will be pivotal in addressing key challenges in organic synthesis, driving synthetic innovation, and enhancing environmental sustainability in the years to come.

## Data availability

All data are stored in the originally, already published papers cited in this Highlight.

## Conflicts of interest

The authors declare no conflict of interest to declare.

## Acknowledgements

C. Q. acknowledges support from China Scholarship Council (202308610077) for a doctoral fellowship. M. L. I. acknowledges



support from the European Union through the EU4Belarus SALT II (Support to Advanced Learning and Training).

## Notes and references

- (a) Y. Fan, S. Li, J. Bao, L. Shi, Y. Yang, F. Yu, P. Gao, H. Wang, L. Zhong and Y. Sun, *Green Chem.*, 2018, **20**, 3450–3456; (b) Y. Wang, Y. He and S. Zhu, *Acc. Chem. Res.*, 2022, **55**, 3519–3536; (c) R. Y. Liu and S. L. Buchwald, *Acc. Chem. Res.*, 2020, **53**, 1229–1243; (d) J. V. Obligation and P. J. Chirik, *Nat. Rev. Chem.*, 2018, **2**, 15–34; (e) S. W. M. Crossley, C. Obradors, R. M. Martinez and R. A. Shenvi, *Chem. Rev.*, 2016, **116**, 8912–9000.
- (a) R. K. Dhungana, S. KC, P. Basnet and R. Giri, *Chem. Rec.*, 2018, **18**, 1314–1340; (b) J. Peng, *Adv. Synth. Catal.*, 2020, **362**, 3059–3080; (c) H. Mei, Z. Yin, J. Liu, H. Sun and J. Han, *Chin. J. Chem.*, 2019, **37**, 292–301; (d) X. Lan, N. Wang and Y. Xing, *Eur. J. Org. Chem.*, 2017, 5821–5851.
- (a) M. Patel, B. Desai, A. Sheth, B. Z. Dholakiya and T. Naveen, *Asian J. Org. Chem.*, 2021, **10**, 3201–3232; (b) G. M. Martins, B. Shirinfar, T. Hardwick and N. Ahmed, *ChemElectroChem*, 2018, **6**, 1300–1315; (c) J. Lin, R. Song, M. Hu and J. Li, *Chem. Rec.*, 2018, **19**, 440–451.
- (a) E. I. Heiba and R. M. Dessau, *J. Am. Chem. Soc.*, 1971, **93**, 995–999; (b) E. Baciocchi, G. Civitarese and R. Ruzziconi, *Tetrahedron Lett.*, 1987, **28**, 5357–5360; (c) K. Narasaka, T. Okauchi, K. Tanaka and M. Murakami, *Chem. Lett.*, 1992, 2099–2102; (d) M.-B. Zhou, R.-J. Song, X.-H. Ouyang, Y. Liu, W.-T. Wei, G.-B. Deng and J.-H. Li, *Chem. Sci.*, 2013, **4**, 2690–2694.
- (a) M. C. White, A. G. Doyle and E. N. Jacobsen, *J. Am. Chem. Soc.*, 2001, **123**, 7194–7195; (b) M. R. Bukowski, P. Comba, A. Lienke, C. Limberg, C. Lopez de Laorden, R. Mas-Ballesté, M. Merz and L. Que, *Angew. Chem., Int. Ed.*, 2006, **45**, 3446–3449; (c) H. Sugimoto, K. Kitayama, S. Mori and S. Itoh, *J. Am. Chem. Soc.*, 2012, **134**, 19270–19280; (d) J.-H. Fan, W.-T. Wei, M.-B. Zhou, R.-J. Song and J.-H. Li, *Angew. Chem., Int. Ed.*, 2014, **53**, 6650–6654; (e) X. Sun, X. Li, S. Song, Y. Zhu, Y.-F. Liang and N. Jiao, *J. Am. Chem. Soc.*, 2015, **137**, 6059–6066.
- (a) A. Frontana-Urbe, R. D. Little, J. G. Ibanez, A. Palma and R. Vasquez-Medrano, *Green Chem.*, 2010, **12**, 2099–2119; (b) M. Yan, Y. Kawamata and P. S. Baran, *Chem. Rev.*, 2017, **117**, 13230–13319; (c) A. Wiebe, T. Gieshoff, S. Möhle, E. Rodrigo, M. Zirbes and S. R. Waldvogel, *Angew. Chem., Int. Ed.*, 2018, **57**, 5594–5619; (d) A. Shatskiy, H. Lundberg and M. D. Kärkäs, *ChemElectroChem*, 2019, **6**, 4067–4092; (e) D. Pollok and S. R. Waldvogel, *Chem. Sci.*, 2020, **11**, 12386–12400; (f) C. Zhu, N. W. J. Ang, T. H. Meyer, Y. Qiu and L. Ackermann, *ACS Cent. Sci.*, 2021, **7**, 415–431; (g) L. F. T. Novaes, J. Liu, Y. Shen, L. Lu, J. M. Meinhardt and S. Lin, *Chem. Soc. Rev.*, 2021, **50**, 7941–8002.
- (a) J.-H. Qin, J.-H. Li and N. Nan, *Synthesis*, 2023, 2843–2859; (b) J. C. Siu, N. Fu and S. Lin, *Acc. Chem. Res.*, 2020, **53**, 547–560; (c) G. S. Sauer and S. Lin, *ACS Catal.*, 2018, **8**, 5175–5187; (d) P. Wang, X. Gao, P. Huang and A. Lei, *ChemCatChem*, 2019, **12**, 27–40.
- (a) E. Steckhan, *Angew. Chem., Int. Ed. Engl.*, 1986, **25**, 683–701; (b) R. Francke and R. D. Little, *Chem. Soc. Rev.*, 2014, **43**, 2492–2521; (c) W. Shao, B. Lu, J. Cao, J. Zhang, H. Cao, F. Zhang and C. Zhang, *Chem. – Asian J.*, 2022, **18**, e202201093.
- (a) C. A. Malapit, M. B. Prater, J. R. Cabrera-Pardo, M. Li, T. D. Pham, T. P. McFadden, S. Blank and S. D. Minter, *Chem. Rev.*, 2021, **122**, 3180–3218; (b) X. Wang, X. Xu, Z. Wang, P. Fang and T. Mei, *Chin. J. Org. Chem.*, 2020, **40**, 3738–3747; (c) W. Zheng, Y. Tao, W. Ma and Q. Lu, *Synthesis*, 2022, 2896–2910; (d) X. Chang, Q. Zhang and C. Guo, *Angew. Chem., Int. Ed.*, 2020, **59**, 12612–12622.
- A. Ogawa and A. J. Boydston, *Chem. Lett.*, 2015, **44**, 10–16.
- J. Li, W. Huang, J. Chen, L. He, X. Cheng and G. Li, *Angew. Chem., Int. Ed.*, 2018, **57**, 5695–5698.
- (a) M. Ošeka, G. Laudadio, N. P. van Leest, M. Dyga, A. de, A. Bartolomeu, L. J. Goofen, B. de Bruin, K. T. de Oliveira and T. Noël, *Chem.*, 2021, **7**, 255–266; (b) M. Laktsevich-Iskryk, A. Krech, M. Fokin, M. Kimm, T. Jarg, T. Noël and M. Ošeka, *J. Flow Chem.*, 2024, **14**, 139–147.
- (a) M. Atobe, H. Tateno and Y. Matsumura, *Chem. Rev.*, 2017, **118**, 4541–4572; (b) T. Noël, Y. Cao and G. Laudadio, *Acc. Chem. Res.*, 2019, **52**, 2858–2869.
- S. Liu, W. Zhao, J. Li, N. Wu, C. Liu, X. Wang, S. Li, Y. Zhu, Y. Liang and X. Cheng, *CCS Chem.*, 2022, **4**, 693–703.
- S. Zhang, L. Li, P. Wu, P. Gong, R. Liu and K. Xu, *Adv. Synth. Catal.*, 2018, **361**, 485–489.
- Y. Ashikari, T. Nokami and J. Yoshida, *J. Am. Chem. Soc.*, 2011, **133**, 11840–11843.
- K. Tabatabaieian, M. Mamaghani, N. O. Mahmoodi and A. Khorshidi, *Catal. Commun.*, 2008, **9**, 416–420.
- (a) C. M. Hudson, M. R. Marzabadi, K. D. Moeller and D. G. New, *J. Am. Chem. Soc.*, 1991, **113**, 7372–7385; (b) D. G. New, Z. Tesfai and K. D. Moeller, *J. Org. Chem.*, 1996, **61**, 1578–1598; (c) A. Sutterer and K. D. Moeller, *J. Am. Chem. Soc.*, 2000, **122**, 5636–5637; (d) F. Tang and K. D. Moeller, *J. Am. Chem. Soc.*, 2007, **129**, 12414–12415; (e) H. Wu and K. D. Moeller, *Org. Lett.*, 2007, **9**, 4599–4602; (f) H.-C. Xu and K. D. Moeller, *J. Am. Chem. Soc.*, 2008, **130**, 13542–13543; (g) R. Krueger, E. Feng, P. Barzova, N. Lieberman, S. Lin and K. D. Moeller, *J. Org. Chem.*, 2024, **89**, 1927–1940.
- P. Xiong, H. Long, J. Song, Y. Wang, J.-F. Li and H.-C. Xu, *J. Am. Chem. Soc.*, 2018, **140**, 16387–16391.
- (a) C. Zhang, *Adv. Synth. Catal.*, 2014, **356**, 2895–2906; (b) J. Shen, L. Li, J. Xu, C. Shen and P. Zhang, *Org. Biomol. Chem.*, 2023, **21**, 2046–2058.
- (a) A. Claraz, T. Courant and G. Masson, *Org. Lett.*, 2020, **22**, 1580–1584; (b) H. I. Jung, Y. Kim and D. Y. Kim, *Org. Biomol. Chem.*, 2019, **17**, 3319–3323; (c) Z. Li, L. Jiao, Y. Sun, Z. He, Z. Wei and W. Liao, *Angew. Chem., Int. Ed.*, 2020, **59**, 7266–7270.
- W. Jud, C. O. Kappe and D. Cantillo, *Chem. – Eur. J.*, 2018, **24**, 17234–17238.
- L. Zhang, G. Zhang, P. Wang, Y. Li and A. Lei, *Org. Lett.*, 2018, **20**, 7396–7399.
- S. Zhang, L. Li, J. Zhang, J. Zhang, M. Xue and K. Xu, *Chem. Sci.*, 2019, **10**, 3181–3185.
- J.-C. Kang, Y.-Q. Tu, J.-W. Dong, C. Chen, J. Zhou, T.-M. Ding, J.-T. Zai, Z.-M. Chen and S.-Y. Zhang, *Org. Lett.*, 2019, **21**, 2536–2540.
- Z. Guan, H. Wang, Y. Huang, Y. Wang, S. Wang and A. Lei, *Org. Lett.*, 2019, **21**, 4619–4622.
- Y. Yuan, Y. Cao, Y. Lin, Y. Li, Z. Huang and A. Lei, *ACS Catal.*, 2018, **8**, 10871–10875.
- Y. Yuan, Y. Chen, S. Tang, Z. Huang and A. Lei, *Sci. Adv.*, 2018, **4**, eaat5312.
- Y. Wang, L. Deng, H. Mei, B. Du, J. Han and Y. Pan, *Green Chem.*, 2018, **20**, 3444–3449.
- L. Sun, Y. Yuan, M. Yao, H. Wang, D. Wang, M. Gao, Y.-H. Chen and A. Lei, *Org. Lett.*, 2019, **21**, 1297–1300.
- A. Petti, M. C. Leech, A. D. Garcia, I. C. A. Goodall, A. P. Dobbs and K. Lam, *Angew. Chem., Int. Ed.*, 2019, **58**, 16115–16118.
- J. Ke, W. Liu, X. Zhu, X. Tan and C. He, *Angew. Chem., Int. Ed.*, 2021, **60**, 8744–8749.
- (a) L. Capaldo and D. Ravelli, *Eur. J. Org. Chem.*, 2017, 2056–2071; (b) M. Galeotti, M. Salamone and M. Bietti, *Chem. Soc. Rev.*, 2022, **51**, 2171–2223; (c) L. Capaldo, D. Ravelli and M. Fagnoni, *Chem. Rev.*, 2021, **122**, 1875–1924; (d) S. Zhang and M. Findlater, *ACS Catal.*, 2023, **13**, 8731–8751; (e) C. Yang, S. Arora, S. Maldonado, D. A. Pratt and C. R. J. Stephenson, *Nat. Rev. Chem.*, 2023, **7**, 653–666.
- T. Siu and A. K. Yudin, *J. Am. Chem. Soc.*, 2002, **124**, 530–531.
- T. Siu, C. J. Picard and A. K. Yudin, *J. Org. Chem.*, 2005, **70**, 932–937.
- M. Okajima, K. Soga, T. Nokami, S. Suga and J. Yoshida, *Org. Lett.*, 2006, **8**, 5005–5007.
- W. Yan, M. Lin, R. D. Little and C.-C. Zeng, *Tetrahedron*, 2017, **73**, 764–770.
- X. Dong, J. L. Roeckl, S. R. Waldvogel and B. Morandi, *Science*, 2021, **371**, 507–514.
- H.-T. Tang, J.-S. Jia and Y.-M. Pan, *Org. Biomol. Chem.*, 2020, **18**, 5315–5333.
- J. D. Haupt, M. Berger and S. R. Waldvogel, *Org. Lett.*, 2018, **21**, 242–245.
- H. Tang, J. R. Vanhoof and D. De Vos, *Green Chem.*, 2022, **24**, 9565–9569.
- K. Yamamoto, N. Kikuchi, T. Hamamizu, H. Yoshimatsu, M. Kuriyama, Y. Demizu and O. Onomura, *ChemElectroChem*, 2019, **6**, 4169–4172.
- D. E. Holst, D. J. Wang, M. J. Kim, I. A. Guzei and Z. K. Wickens, *Nature*, 2021, **596**, 74–79.
- X.-A. Liang, L. Niu, S. Wang and A. Lei, *Chem. Catal.*, 2021, **1**, 1055–1064.



- 45 Y.-C. Luo, X.-J. Pan and G.-Q. Yuan, *Tetrahedron*, 2015, **71**, 2119–2123.
- 46 A. O. Terent'ev, O. M. Mulina, D. A. Pirgach, A. I. Ilovaisky, M. A. Syroeshkin, N. I. Kapustina and G. I. Nikishin, *Tetrahedron*, 2017, **73**, 6871–6879.
- 47 M. N. Elinson, S. K. Feducovich, Z. A. Starikova, O. S. Olessova, A. N. Vereshchagin and G. I. Nikishin, *Tetrahedron Lett.*, 2000, **41**, 4937–4941.
- 48 A. Krech, M. Laktsevich-Iskryk, N. Deil, M. Fokin, M. Kimm and M. Ošeka, *Chem. Commun.*, 2024, **60**, 14026–14029.
- 49 Z. Wu, S. Li and H. Xu, *Angew. Chem., Int. Ed.*, 2018, **57**, 14070–14074.
- 50 For seminal examples in the field of electrochemical polymerization of olefins: (a) A. J. D. Magenau, N. C. Strandwitz, A. Gennaro and K. Matyjaszewski, *Science*, 2011, **332**, 81–84; (b) B. Li, B. Yu, W. T. S. Huck, F. Zhou and W. Liu, *Angew. Chem., Int. Ed.*, 2012, **51**, 5092–5095; (c) N. Shida, Y. Koizumi, H. Nishiyama, I. Tomita and S. Inagi, *Angew. Chem., Int. Ed.*, 2015, **54**, 3922–3926; (d) M. Fantin, A. A. Isse, A. Venzo, A. Gennaro and K. Matyjaszewski, *J. Am. Chem. Soc.*, 2016, **138**, 7216–7219.
- 51 B. M. Peterson, S. Lin and B. P. Fors, *J. Am. Chem. Soc.*, 2018, **140**, 2076–2079.
- 52 N. Fu, G. S. Sauer, A. Saha, A. Loo and S. Lin, *Science*, 2017, **357**, 575–579.
- 53 N. Fu, G. S. Sauer and S. Lin, *J. Am. Chem. Soc.*, 2017, **139**, 15548–15553.
- 54 K. Ye, Z. Song, G. S. Sauer, J. H. Harenberg, N. Fu and S. Lin, *Chem. – Eur. J.*, 2018, **24**, 12274–12279.
- 55 N. Fu, Y. Shen, A. R. Allen, L. Song, A. Ozaki and S. Lin, *ACS Catal.*, 2019, **9**, 746–754.
- 56 J. Sim, B. Ryou, M. Choi, C. Lee and C.-M. Park, *Org. Lett.*, 2022, **24**, 4264–4269.
- 57 For reviews on C–H activation and functionalization strategies, see: (a) H. M. L. Davies, J. Du Bois and J.-Q. Yu, *Chem. Soc. Rev.*, 2011, **40**, 1855–1856 and related thematic issue; ; (b) T. W. Lyons and M. S. Sanford, *Chem. Rev.*, 2010, **110**, 1147–1169; (c) T. Dalton, T. Faber and F. Glorius, *ACS Cent. Sci.*, 2021, **7**, 245–261; (d) M. Moselage, J. Li and L. Ackermann, *ACS Catal.*, 2015, **6**, 498–525.
- 58 For reviews on metallaelectrocatalysis: (a) L. Ackermann, *Acc. Chem. Res.*, 2019, **53**, 84–104; (b) P. Gandeepan, L. H. Finger, T. H. Meyer and L. Ackermann, *Chem. Soc. Rev.*, 2020, **49**, 4254–4272; (c) N. Sauermann, T. H. Meyer and L. Ackermann, *Chem. – Eur. J.*, 2018, **24**, 16209–16217.
- 59 T. H. Meyer, J. C. A. Oliveira, S. C. Sau, N. W. J. Ang and L. Ackermann, *ACS Catal.*, 2018, **8**, 9140–9147.
- 60 Y. Lin, T. von Münchow and L. Ackermann, *ACS Catal.*, 2023, **13**, 9713–9723.
- 61 Y. Li, J. Xu, J. C. A. Oliveira, A. Scheremetjew and L. Ackermann, *ACS Catal.*, 2024, **14**, 8160–8167.
- 62 X. Huang, Q. Zhang, J. Lin, K. Harms and E. Meggers, *Nat. Catal.*, 2018, **2**, 34–40.
- 63 E. B. Bauer, *Chem. Soc. Rev.*, 2012, **41**, 3153–3167.
- 64 P. Xiong, M. Hemming, S. I. Ivlev and E. Meggers, *J. Am. Chem. Soc.*, 2022, **144**, 6964–6971.
- 65 J. M. Lassaletta, *Nat. Commun.*, 2020, **11**, 3787.
- 66 D. Mazzarella, C. Qi, M. Vanzella, A. Sartorel, G. Pelosi and L. Dell'Amico, *Angew. Chem., Int. Ed.*, 2024, **63**, e202401361.
- 67 B. L. Truesdell, T. B. Hamby and C. S. Sevov, *J. Am. Chem. Soc.*, 2020, **142**, 5884–5893.

